Open-system dynamics and mixing in magma mushes

G. W. Bergantz[1]*, J. M. Schleicher[1] and A. Burgisser[2]

Magma dominantly exists in a slowly cooling crystal-rich or mushy state[1-3]. Yet, observations of complexly zoned crystals[4], some formed in just one to ten years[5-9], as well as time-transgressive crystal fabrics[10] imply that magmas mix and transition rapidly from a locked crystal mush to a mobile and eruptable fluid[5,6]. Here we use a discrete-element numerical model that resolves crystal-scale granular interactions and fluid flow, to simulate the open-system dynamics of a magma mush. We find that when new magma is injected into a reservoir from below, the existing magma responds as a viscoplastic material: fault-like surfaces form around the edges of the new injection creating a central mixing bowl of magma that can be unlocked and become fluidized, allowing for complex mixing. We identify three distinct dynamic regimes that depend on the rate of magma injection. If the magma injection rate is slow, the intruded magma penetrates and spreads by porous media flow through the crystal mush. With increasing velocity, the intruded magma creates a stable cavity of fluidized magma that is isolated from the rest of the reservoir. At higher velocities still, the entire mixing bowl becomes fluidized. Circulation within the mixing bowl entrains crystals from the walls, bringing together crystals from different parts of the reservoir that may have experienced different physiochemical environments and leaving little melt unmixed. We conclude that both granular and fluid dynamics, when considered simultaneously, can explain observations of complex crystal fabrics and zoning observed in many magmatic systems.

The transport of heat and mass from the Earth's deep interior to the surface by magmatism (volcanism) creates the Earth's crust and strongly conditions the atmosphere and biosphere. Geochemical and geophysical observations have converged to a view of magma systems existing in a mushy and quasi-static state for much of their thermal lifetime. Yet they have a contradictory nature: slow cooling under crystal-rich conditions, yet punctuated by rapid mixing, sometimes just before eruption[11,12]. This has been documented from ocean islands and large igneous provinces[13,14], to convergent margin volcanic systems[2,5,6], to mid-ocean ridge systems[9] and inferred for magmatic systems on Mars[15]. This is typically expressed by the occurrence of populations of complexly zoned crystals[4] and time-transgressive crystal fabrics in plutons[10].

To illuminate the combined fluid and granular behaviour of crystal-rich magmas, we have performed discrete element–computational fluid dynamics (DEM–CFD) numerical simulations of a crystal mush. This approach explicitly considers frictional, collisional, translational, buoyant, lubrication and viscous particle–particle–fluid coupling at the crystal scale. This allows us to recover multiphase dynamics from a contact stress-chain supported framework with porous flow to fully fluid behaviour simultaneously,

without the *ad hoc* assumptions of a mixture theory or other continuum methods. We model a crystal mush of basaltic composition, as these are widespread on Earth and Mars, and where the processes are most simply exemplified. The model is composed of a bed of crystals, with the properties of olivine in a larger basaltic liquid reservoir (Fig. 1a). The mush was populated with crystals that have naturally settled with about 40% residual porosity. At the start of the simulation, new, crystal-free magma is intruded as a dyke at the bottom of the resident mush. The evolution of the subsequent mixing between the resident mush and the new magma by penetrative convection and granular interactions is described and quantified in Fig. 1, and a computer simulation is archived in Supplementary file V1.

Initially, the crystal mush is supported by crystal–crystal contacts forming random, vertically directed stress chains. When new, intruding magma encounters the resident crystal mush, the mush pile responds initially as a viscoplastic medium. This leads to the rotation of the dominant direction of the stress chains and the appearance of two conjugate failure surfaces or faults, whose orientation is approximately 60° to the horizontal, as predicted by the Mohr–Coulomb failure criteria (Fig. 1a). These faults delimit the volume of the mush that can be subsequently unlocked, or fluidized by increases in pore pressure. We call this region the 'mixing bowl.' The lateral scale of the mixing bowl is largely fixed, although there is minor erosion and crystal–crystal translation along the fault surfaces, piling-up of crystals at the top and minor lateral porous leakage of new melt. Under high-temperature conditions the faults could evolve into mylonites and produce repeating localized shear bands and crystal fabrics as observed in mid-ocean ridge and granitic plutonic rocks[10,16,17].

If the mass flux of new magma is sufficiently high, the centre of the mixing bowl is fluidized and occupied by the largest-scale dynamic features: the central conduit or chimney, and 'granular vortices' (Fig. 1b,c). The central chimney is the locus for the new magma traversing the resident crystal mush. Once new magma encounters the fluidized crystal mush, the central chimney bifurcates in a pulsating fashion. This sets the initial length scale for the chimney; however, the diameter of the central chimney is not simply recovered by either Rayleigh–Taylor or Saffman–Taylor viscous fingering scaling[18]. Once established, the circulation in the mixing bowl persists as a fixed, or self-similar, kinematic template, and if the input mass flux and associated Reynolds number is high enough the chimney undergoes both varicose and meandering instabilities[19,20]. As the penetrative convection of new magma transits the mixing bowl, crystals and resident melt are entrained from the walls and transported upwards in the chimney. Once expelled from the chimney they travel along the mush–reservoir interface by slumping and crystal-rich avalanches.

[1]Department of Earth and Space Sciences, Box 351310, University of Washington, Seattle, Washington 98195, USA. [2]Institut des Sciences de la Terre, CNRS—IRD—Université de Savoie, Campus Scientifique, 73376 Le Bourget du Lac, France. *e-mail: bergantz@uw.edu
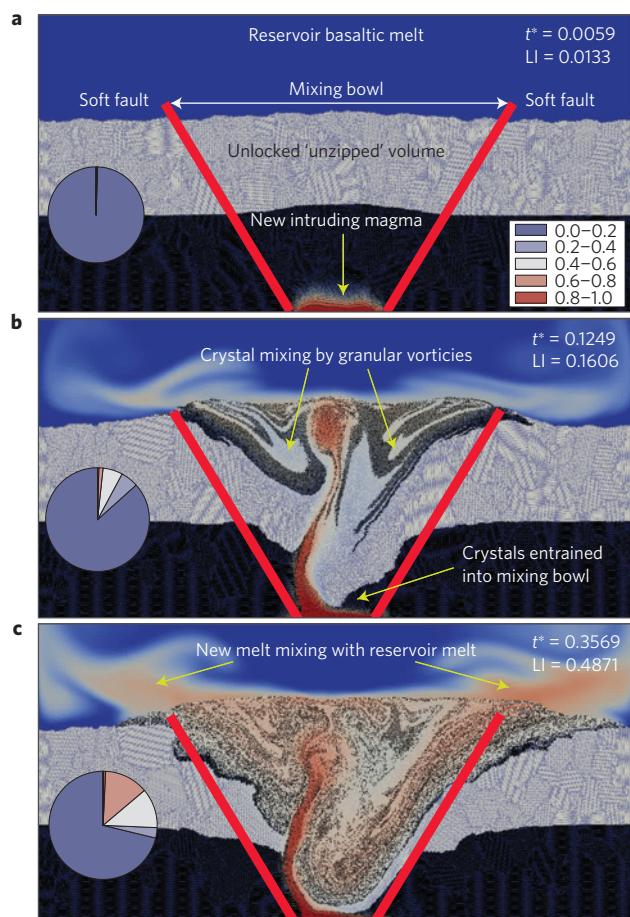
Figure 1 | Three time steps from the simulation of an open-system event in basaltic mush. Computer simulation is archived as Supplementary file V1. The settled crystals are identical, and are coloured black and white for visualization. The basaltic liquid is blue. The new magma is red and the dimensionless velocity U^* is 9.3. Pie charts indicate the percentage of crystals residing in different melt compositions. The resident (blue), and new (red), magma are represented by 0.0 and 1.0, respectively. **a**, Formation of the mixing bowl by viscoplastic failure of the mush along two conjugate granular faults. **b**, Continued input unlocks the mixing bowl and entrains a crystal cargo from the bottom and core of the mush. **c**, Continued input induces circulation.

This erosion, transport and mixing of resident melt, crystals and new melt is so efficient that little of the new melt exits the chimney unmixed, and it is laterally and vertically dispersed in the crystal-free reservoir (Fig. 1c).

Upward flow in the central chimney sustains intermittent counter-rotating granular vortices in the widest part of the mixing bowl. This rotating motion, regular at low Reynolds number, or irregular at higher Reynolds number, dominates material advection away from the chimney. The uppermost regions of these vortices are composed of crystals recently deposited after transit from the bottom or middle region of the crystal pile. This brings together crystals that may have experienced and recorded very different physicochemical environments (Fig. 2a,b). These newly deposited crystals have a loose packing that is supported by their crystal–melt–crystal contacts and creates local gradients in porosity. This enhanced porosity allows for secondary infiltration and mixing by new melt. As these crystals are rotated downward by the vortices, the crystal packing increases and interstitial melt is forced radially away from the centre of rotation. This process acts as a secondary source of new melt advected into the distal parts of the mixing bowl.
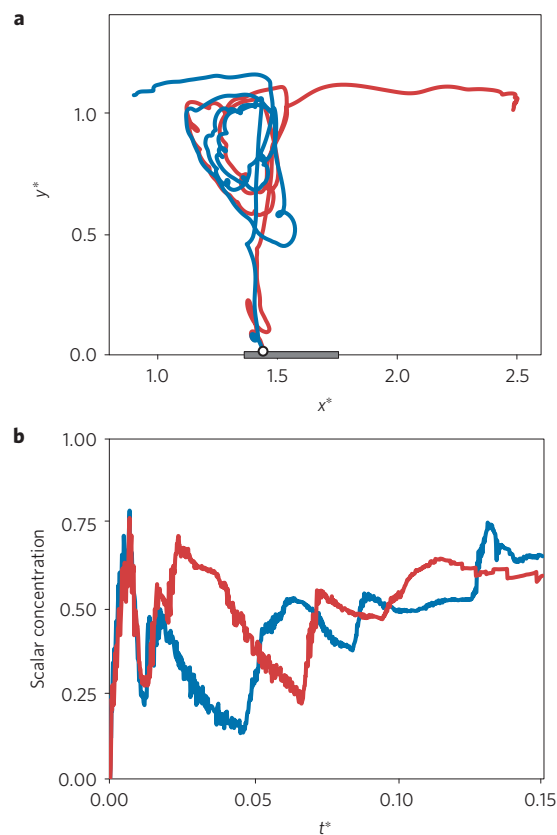

Figure 2 | Crystal trajectories and zoning. a, Trajectories of two crystals that originate from a common location, illustrating complex crystal dispersal and gathering. The grey strip in the bottom centre is the location of new magma input and provides scale. **b**, Concentration of the melt that the two crystals in **a** encounter during transport. This can be considered a synthetic crystal zoning record.

Distinct time-dependent states of an open-system event can be rationalized by the definition of a dimensionless velocity for the system. We define a dimensionless velocity U^* that is normalized relative to the minimum fluidization velocity U_{mf}, or mass flux, for the volume of the mixing bowl[21]; the scaled velocity U^* can be thought of as the excess momentum flux over that required for incipient fluidization. If the intruding magma has a U^* less than unity the mush is not fluidized and two other distinct self-similar states have been recovered and confirmed by physical experiments[22] (not shown here). At values of U^* well below unity, the incoming new magma is unable to fluidize or create enhanced porosity by over-pressure, and so new melt infiltrates the resident mush by Darcian porous flow and spherical spreading, as preserved in geologic examples from Iceland[23]. As U^* is increased pore pressure produces a local unlocking of the resident mush and allows for the formation of a stable cavity within the mush that does not penetrate the entire mush pile. This cavity acts as a melt staging area, and new magma seeps into the core of the mixing bowl; however, this process is still rate-limited by porous flow. Hence, we recognize three distinct self-similar regimes: at $U^* \ll 1$, new magma penetrates the resident mush only by porous flow; at $U^* < 1$, a stable cavity forms within the mush with subsequent delivery again by porous flow; and at $U^* \geq 1$, the entire mixing bowl is fluidized and large-scale vertical motions obtained (Fig. 1).

Next we will address the mixing of the resident crystals (self-mixing[24]) within the crystal pile. To quantify crystal–crystal mixing we have used the Lacey index[25] (LI), see Supplementary Information. The LI provides a single estimate of the particle mixedness for
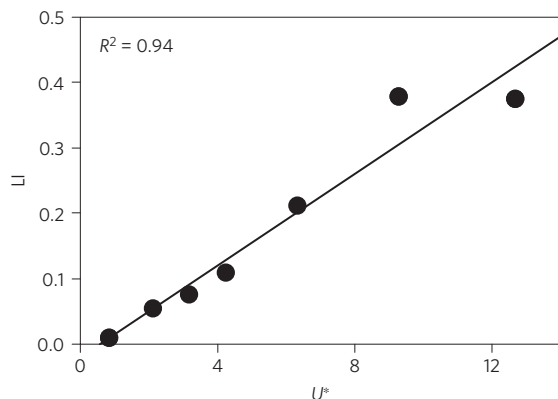
Figure 3 | Crystal–crystal mixing efficiency. LI or goodness of crystal–crystal mixing as a function of scaled velocity U^* at t^* equal to 0.238. These results demonstrate that a self-similar regime is established for a range of U^* once the mixing bowl is fully fluidized.

the entire domain and varies from a value of zero for a perfectly segregated mixture to unity for a perfectly random 'well mixed' state. It can be thought of as the mixing achieved relative to the mixing possible. It is the variance within the mixing domain of the concentration of the partially mixed particles minus the variance in the unmixed domain, divided by the variances of the randomly mixed domain minus the unmixed domain. Figure 3 shows the dependence of LI as a function of U^*. Note that it is linear. This exposes the influence of the elliptic points, or attractors, in the template of circulation created by the granular vortices within the mixing bowl.

Individual crystals reveal a more complex story. This is shown in Fig. 2 by following a pair of randomly chosen crystals, which are adjacent at the start of the simulation. In Fig. 2a, their respective trajectories are plotted and the tendency for dispersal and gathering of crystals is manifest. In Fig. 2b, the same two crystals are shown as a function of dimensionless time, t^*, which is defined as $(U_{mf}/H_o)t$, where H_o is the original bed height and t is time. Their 'flight recorders' download the local value of a tracer scalar that is a proxy for liquid concentration of the new magma. This illustrates how the common occurrence of complex crystal zoning arises by advection through regions of distinct chemical potential, which themselves are simultaneously being mixed and dissipated. Natural examples rarely seem to have such high-frequency chemical oscillations. This is the result of chemical kinetics, absent in our simulations, which will act as a low-pass filter producing time delay and diminishing the amplitude of the crystal-chemical response. Nonetheless, the simulated zoning captures some of the long-wavelength features commonly observed in the crystal cargo of mixed magmas[26,27] and confirms that complex crystal zoning is an expected consequence of simultaneous crystal and melt mixing even under very simple open-system conditions.

Complex yet rapid mixing of magmatic mushes is widely encountered yet poorly understood[2]. We have demonstrated the role of granular processes as expressed by pore pressure, crystal–crystal and crystal–melt interactions, and viscoplastic behaviour, in preconditioning magma mushes for mechanical unlocking and establishing the initial mixing volume. During fluidization and mixing, ephemeral crystal stress-chain interactions and non-affine deformation allow for strain localization and a variety of mixing conditions to coexist. The resolution of the DEM–CFD method reveals the limitations of traditional approaches of magma dynamics based solely on continuum assumptions of fluid behaviour augmented by suspension rheology. Magmatic systems with large viscosity variations and multi-modal crystal populations are predicted to show even more complexity[28] and DEM–CFD is a promising technology for probing their mechanics.

Methods

Methods and any associated references are available in the online version of the paper.

References

1. Hayes, B., Bédard, J. H. & Lissenberg, C. J. Olivine slurry replenishment and the development of igneous layering in a Franklin Sill, Victoria Island, Arctic Canada. *J. Petrol.* **56,** 83–112 (2015).
2. Cassidy, M., Edmonds, M., Watt, S. F. L., Palmer, M. R. & Gernon, T. M. Origin of basalts by hybridization in andesite-dominated arcs. *J. Petrol.* **56,** 325–346 (2015).
3. Ward, K. M., Zandt, G., Beck, S. L., Christensen, D. H. & McFarlin, H. Seismic imaging of the magmatic underpinnings beneath the Altiplano-Puna volcanic complex from the joint inversion of surface wave dispersion and receiver functions. *Earth Planet. Sci. Lett.* **404,** 43–53 (2014).
4. Kahl, M., Chakraborty, S., Costa, F. & Pompilio, M. Dynamic plumbing system beneath volcanoes revealed by kinetic modeling, and the connection to monitoring data: An example from Mt. Etna. *Earth Planet. Sci. Lett.* **308,** 11–22 (2011).
5. Cooper, K. M. & Kent, A. J. R. Rapid remobilization of magmatic crystals kept in cold storage. *Nature* **506,** 480–483 (2014).
6. Klemetti, E. W. & Clynne, M. A. Localized rejuvenation of a crystal mush recorded in zircon temporal and compositional variation at the Lassen volcanic center, northern California. *PLoS ONE* **9,** e113157 (2014).
7. Barboni, M. & Schoene, B. Short eruption window revealed by absolute crystal growth rates in a granitic magma. *Nature Geosci.* **7,** 524–528 (2014).
8. Passmore, E., Maclennan, J., Fitton, G. & Thordarson, T. Mush disaggregation in basaltic magma chambers: Evidence from the AD 1783 Laki eruption. *J. Petrol.* **53,** 2593–2623 (2012).
9. Costa, F., Coogan, L. A. & Chakraborty, S. The time scales of magma mixing and mingling involving primitive melts and melt–mush interaction at mid-ocean ridges. *Contrib. Mineral. Petrol.* **159,** 371–387 (2010).
10. Paterson, S. R. Magmatic tubes, pipes, troughs, diapirs, and plumes: Late-stage convective instabilities resulting in compositional diversity and permeable networks in crystal-rich magmas of the Tuolumne batholith, Sierra Nevada, California. *Geosphere* **5,** 496–527 (2009).
11. Burgisser, A. & Bergantz, G. W. A rapid mechanism to remobilize and homogenize highly crystalline magma bodies. *Nature* **471,** 212–215 (2011).
12. Huber, C., Bachmann, O. & Dufek, J. Thermo-mechanical reactivation of locked crystal mushes: Melting-induced internal fracturing and assimilation processes in magmas. *Earth Planet. Sci. Lett.* **304,** 443–454 (2011).
13. Zieg, M. J. & Marsh, B. D. Multiple reinjections and crystal-mush compaction in the beacon sill, McMurdo Dry Valleys, Antarctica. *J. Petrol.* **53,** 2567–2591 (2012).
14. Neave, D. A., Passmore, E., Maclennan, J., Fitton, G. & Thordarson, T. Crystal-melt relationships and the record of deep mixing and crystallization in the AD 1783 Laki eruption, Iceland. *J. Petrol.* **54,** 1661–1690 (2013).
15. Ehlmann, B. L. & Edwards, C. S. Mineralogy of the Martian surface. *Annu. Rev. Earth Planet. Sci.* **42,** 291–315 (2014).
16. Mehl, L. & Hirth, G. Plagioclase preferred orientation in layered mylonites: Evaluation of flow laws for the lower crust. *J. Geophys. Res.* **113,** B05202 (2008).
17. Paterson, S. R., Žák, J. & Janoušek, V. Growth of complex sheeted zones during recycling of older magmatic units into younger: Sawmill Canyon area, Tuolumne batholith, Sierra Nevada, California. *J. Volcanol. Geotherm. Res.* **177,** 457–484 (2008).
18. Bischofberger, I., Ramachandran, R. & Nagel, S. R. Fingering versus stability in the limit of zero interfacial tension. *Nature Commun.* **5,** 5265 (2014).
19. Huppert, H. E., Sparks, R. S. J., Whitehead, J. A. & Hallworth, M. A. Replenishment of magma chambers by light inputs. *J. Geophys. Res.* **91,** 6113–6122 (1986).
20. Dombrowski, C. *et al.* Coiling, entrainment, and hydrodynamic coupling of decelerated fluid jets. *Phys. Rev. Lett.* **95,** 184501 (2005).
21. Peng, Y. & Fan, L. T. Hydrodynamic characteristics of fluidization in liquid-solid tapered beds. *Chem. Eng. Sci.* **52,** 2277–2290 (1997).
22. Philippe, P. & Badiane, M. Localized fluidization in a granular medium. *Phys. Rev. E* **87,** 042206 (2013).
23. Thomson, A. & Maclennan, J. The distribution of olivine compositions in Icelandic basalts and picrites. *J. Petrol.* **54,** 745–768 (2013).
24. Couch, S., Sparks, R. S. J. & Caroll, M. R. Mineral disequilibrium in lavas explained by convective self-mixing in open magma chambers. *Nature* **411,** 1037–1039 (2001).
25. Lacey, P. M. C. Developments in the theory of particle mixing. *J. Appl. Chem.* **4,** 257–268 (1954).

26. Wallace, G. S. & Bergantz, G. W. Reconciling heterogeneity in crystal zoning data: An application of shared characteristic diagrams at Chaos Crags, Lassen volcanic center, California. *Contrib. Mineral. Petrol.* **149,** 98–112 (2005).
27. Ruprecht, P., Bergantz, G. W. & Dufek, J. Modeling of gas-driven magmatic overturn: Tracking of phenocryst dispersal and gathering during magma mixing. *Geochem. Geophys. Geosyst.* **9,** Q07017 (2008).
28. Laumonier, M. *et al.* On the conditions of magma mixing and its bearing on andesite production in the crust. *Nature Commun.* **5,** 5607 (2014).

Author contributions

G.W.B. wrote the manuscript and directed the numerical experiments. J.M.S. performed the simulations, created the figures and contributed to the Supplementary Information. A.B. contributed to the performance of the simulations. All authors participated in the workflow and revisions.

Additional information

Supplementary information is available in the online version of the paper. Reprints and permissions information is available online at www.nature.com/reprints. Correspondence and requests for materials should be addressed to G.W.B.

Competing financial interests

The authors declare no competing financial interests.

Methods

We performed simulations using a modified version of the MFIX (Multiphase Flow with Interphase eXchange) numerical algorithm developed by the United States Department of Energy supported National Energy and Technology Laboratory. It simulates multiphase flow employing the discrete element method–computational fluid dynamics (DEM–CFD). This is a Lagrangian–Eulerian approach for solid and fluid phases where the method allows us to model particle–particle and hydrodynamic interactions with 4-way coupling. Collisions, sustained frictional contact, buoyancy, fluid drag and interphase momentum transport between phases are modelled with the soft-sphere approach, using a spring–dashpot system to model the contact and hydrodynamic forces[29]. Additional details related to the Lagrangian particle physics can be found in the documentation of the MFIX-DEM algorithm[30], the multiphase theory and implementation are discussed in the Supplementary Information.

A discussion of validation, verification and the sensitivity to choice of DEM contact parameters is provided in the Supplementary Information.

The domain is initialized with a settled bed of particles (crystals) within a fluid (magma)-filled domain. Within the bed, the pore space is initially filled by magma coloured blue, giving an average fluid-volume fraction of ∼0.4. Magma injected into the domain from the base is coloured red, and mixing between it and the resident magma is shown as a gradient from blue to red. Conservation of mass and pressure relief is provided by mass flow through the upper boundary. Solid boundaries have a no-slip boundary condition for the fluid and a wall-friction law for the crystals, but most fluid and particle motion occurs far from the walls, so boundary conditions have little influence on the dynamics. Crystals are coloured black and white to indicate their initial position within either the bottom or top half of the domain; otherwise their physical properties are identical.

For the simulation of a basaltic system we have ignored the effects of temperature as it is commonly observed that crystal-rich basaltic eruptions are thermally buffered; that is, there are very minor changes in temperature for eruptions from the same system occurring repeatedly over decades. We have also treated the thermophysical and transport properties such as viscosity and density as constant, as they vary little in a thermally buffered basaltic environment and where the differences in local particle volume fraction dominate the mixture properties relative to changes in fluid properties alone. We have also not considered the role of bubbles, as mixing is commonly observed in magma systems that cooled at pressures where volatile exsolution occurs well after mushy conditions are obtained.

Code availability. The code used to produce the DEM–CFD is publicly available at http://mfix.netl.doe.gov.

References

29. Cundall, P. A. & Strack, O. D. L. A discrete numerical model for granular assemblies. *Géotechnique* **29,** 47–65 (1979).
30. Garg, R., Galvin, J., Li, T. & Pannala, S. *Documentation of Open-Source MFIX-DEM Software for Gas-Solids Flows* (Department of Energy, National Energy Technology Laboratory, 2012); https://mfix.netl.doe.gov/download/mfix/mfix_current_documentation/dem_doc_2012-1.pdf